PAPER

Parallelization of Boost and Buck Type DC-DC Converters by Individual Passivity-Based Control

Yuma MURAKAWA[†a)], ***Student Member***, **Yuhei SADANDA**[†b)], ***Nonmember***, ***and*** **Takashi HIKIHARA**[†c)], ***Fellow***

SUMMARY This paper discusses the parallelization of boost and buck converters. Passivity-based control is applied to each converter to achieve the asymptotic stability of the system. The ripple characteristics, error characteristics, and time constants of the parallelized converters are discussed with considering the dependency on the feedback gains. The numerical results are confirmed to coincide with the results in the experiment for certain feedback gains. The stability of the system is also discussed in simulation and experiment. The results will be a step to achieve the design of parallel converters.

key words: *parallelization, DC-DC converter, passivity-based control, distributed power source*

1. Introduction

In recent years, distributed power sources, such as solar cells and batteries, have actively been studied [1], [2]. It is tightly related to the global demand for clean energy. These sources tend to have a relatively small and limited amount of output. Cooperative use of various power sources may realize distributed generation [3], [4]. Power converters play a very important role as interfaces for them.

The parallelization of power converters has widely been discussed for the past two decades [5]. There have been works that focus on obtaining a larger power capacity by sharing the load current equally between parallelized converters. However, the parallel connection of different converters nor obtaining uneven current distribution has not been a subject of study. The multiple-input DC-DC converter is considered in [6] for the combination of various power sources. The generalized argument of such a system has not been accomplished though.

The connection of different power sources and converters will make the system complexed. The control method based on the knowledge of the whole system is unrealistic. Decentralized control and design are necessary for the scalability and diversity of the system. Therefore, passivity-based control (PBC) is proposed [7]. The control method keeps the advantage of the passive characteristics which inherently physical systems have. It aims to stabilize the system by modifying the energy function. The application of PBC to DC-DC converters was given in [8]. More generalized arguments were well explained in [9], [10].

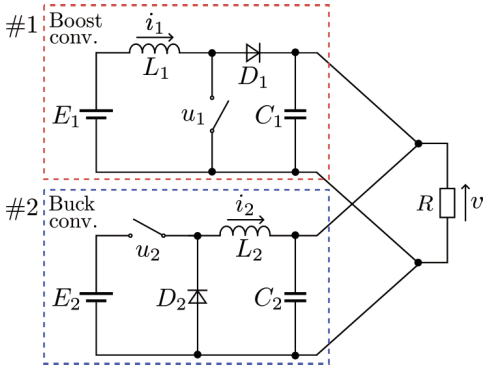

Fig. 1 Schematic circuit of parallelized boost and buck converters.

An electric circuit composed of passive elements is known to be passive [11]. Hence, by applying PBC to the converters individually and assuring each energy function to be asymptotically stable, it is expected that the parallelized system will also be asymptotically stable. From this perspective, the stabilization of Ćuk converters connected in parallel by PBC is discussed in [12]. The application of PBC is extended to ring coupled boost converters [13].

This paper focuses on parallelizing two different types of DC-DC converters; boost and buck. They are one of the most major converters which are used in many types of electrical equipment. Boost and buck converters have the function of stepping the voltage up and down, respectively. Therefore, the parallelization of these converters enables the combination of a wide variety of power sources with various output voltages. Here, PBC is introduced to each converter individually. Their characteristics are explored numerically and experimentally. In Sect. 2, we will analytically show that the individual PBC assures the whole parallelized system to be asymptotically stable. Sections 3 and 4 are devoted to the numerical and experimental confirmation, respectively. Section 5 is the conclusion.

2. Parallelization of Boost and Buck Converters and Application of Passivity-Based Control

Figure 1 is a schematic circuit of parallelized boost and buck converters. The converters are sharing a load at the output. Each converter consists of voltage source E, load R, inductance L, capacitance C, switch u, and diode D. Here, i denotes the inductor current and v the capacitor voltage.

Manuscript received May 13, 2019.
Manuscript revised October 24, 2019.

[†]The authors are with the Department of Electrical Engineering, Kyoto University, Kyoto-shi, 615-8510 Japan.
a) E-mail: y-murakawa@dove.kuee.kyoto-u.ac.jp
b) E-mail: y-sadanda@dove.kuee.kyoto-u.ac.jp
c) E-mail: hikihara.takashi.2n@kyoto-u.ac.jp

DOI: 10.1587/transfun.2019EAP1069

The subscripts '1' and '2' correspond to converter #1 (boost converter) and converter #2 (buck converter), respectively. Note that all circuit elements mentioned in this section are ideal.

2.1 System Model

The Kirchhoff's laws give the differential equations of the parallelized circuit shown in Fig. 1 as

$$\begin{cases} L_1\dot{i}_1 = -(1-u_1)v + E_1, \\ L_2\dot{i}_2 = -v + u_2E_2, \\ C_{12}\dot{v} = (1-u_1)i_1 + i_2 - \dfrac{v}{R}, \end{cases} \tag{1}$$

where $C_{12} = C_1 + C_2$. The dot $(\dot{})$ on the variable is a notation for time differentiation. The system is discontinuous with the switching variables $u_1, u_2 \in \{0, 1\}$, switching the system structure. Regulation of power converters implies switching operation, which corresponds to the switching variables u_1 and u_2.

Assuming a high frequency switched pulse width modulation (PWM), the state averaging model of DC-DC converters is obtained [8], [14]. By averaging Eq. (1), we obtain

$$\begin{cases} L_1\dot{i}_1 = -(1-\mu_1)v + E_1, \\ L_2\dot{i}_2 = -v + \mu_2E_2, \\ C_{12}\dot{v} = (1-\mu_1)i_1 + i_2 - \dfrac{v}{R}. \end{cases} \tag{2}$$

The switching variables u_1, u_2 are replaced with duty ratios $\mu_1, \mu_2 \in [0, 1]$.

Control objective, here, would be obtaining the asymptotical stability at the desired state $[i_1,\ i_2,\ v] = [i_{1\mathrm{d}},\ i_{2\mathrm{d}},\ v_{\mathrm{d}}]$, by modifying the duty ratios μ_1 and μ_2. Null curve of Eq. (2) is obtained as

$$\begin{cases} \mu_1 = 1 - \dfrac{E_1}{v}, \\ \mu_2 = \dfrac{v}{E_2}, \\ E_1i_1 + \mu_2E_2i_2 = \dfrac{v^2}{R}. \end{cases} \tag{3}$$

The desired state $[i_1\, i_2\, v] = [i_{1\mathrm{d}}\, i_{2\mathrm{d}}\, v_{\mathrm{d}}]$ must be chosen to satisfy Eq. (3). The steady state implies that all input energy is consumed at the load, and a specific duty ratio will be chosen for a specific output voltage. Thus the desired duty ratios become

$$\begin{cases} \mu_{1\mathrm{d}} = 1 - \dfrac{E_1}{v_{\mathrm{d}}}, \\ \mu_{2\mathrm{d}} = \dfrac{v_{\mathrm{d}}}{E_2}, \end{cases} \tag{4}$$

which correspond to the desired output order v_{d}.

2.2 Application of Passivity-Based Control

Viewing the parallelized system as a whole, it may adopt several control schemes, for example, approximate linearization and state feedback. However, such an approach is the lack of scalability; the capability of parallelizing more converters. It is natural that decentralized control technique is adopted to focus on each converter. PBC is applied to each converter to assure the stability of the parallelized system.

PBC for each converter are given by

$$\begin{cases} \mu_1 = \mu_{1\mathrm{d}} - k_1(v_{\mathrm{d}}i_1 - vi_{1\mathrm{d}}) & (k_1 > 0), \\ \mu_2 = \mu_{2\mathrm{d}} - k_2(i_2 - i_{2\mathrm{d}}) & (k_2 > 0), \end{cases} \tag{5}$$

whose derivation is defined in the appendix. The shaped storage functions for each converter are

$$\begin{cases} \mathcal{H}_1(i_1,\ v) = \dfrac{1}{2}L_1(i_1 - i_{1\mathrm{d}})^2 + \dfrac{1}{2}C_1(v - v_{\mathrm{d}})^2, \\ \mathcal{H}_2(i_2,\ v) = \dfrac{1}{2}L_2(i_2 - i_{2\mathrm{d}})^2 + \dfrac{1}{2}C_2(v - v_{\mathrm{d}})^2. \end{cases} \tag{6}$$

Then, the storage function $\mathcal{H}_{12}$ for the whole system is their summation

$$\begin{aligned} \mathcal{H}_{12}(i_1,\ i_2,\ v) &= \mathcal{H}_1(i_1,\ v) + \mathcal{H}_2(i_2,\ v) \\ &= \frac{1}{2}L_1(i_1 - i_{1\mathrm{d}})^2 + \frac{1}{2}L_2(i_2 - i_{2\mathrm{d}})^2 + \frac{1}{2}C_{12}(v - v_{\mathrm{d}})^2. \end{aligned} \tag{7}$$

The stability of the desired state $[i_1\, i_2\, v] = [i_{1\mathrm{d}}\, i_{2\mathrm{d}}\, v_{\mathrm{d}}]$ is theoretically examined by the Lyapunov stability theory [15]. Differentiating the desired storage function gives

$$\begin{aligned} \frac{\mathrm{d}\mathcal{H}_{12}}{\mathrm{d}t} &= \frac{\partial\mathcal{H}_{12}}{\partial i_1}\frac{\mathrm{d}i_1}{\mathrm{d}t} + \frac{\partial\mathcal{H}_{12}}{\partial i_2}\frac{\mathrm{d}i_2}{\mathrm{d}t} + \frac{\partial\mathcal{H}_{12}}{\partial v}\frac{\mathrm{d}v}{\mathrm{d}t} \\ &= (\mu_1 - \mu_{1\mathrm{d}})\,(v_{\mathrm{d}}i_1 - vi_{1\mathrm{d}}) + (\mu_2 - \mu_{2\mathrm{d}})\,E(i_2 - i_{2\mathrm{d}}) \\ &\quad - \frac{(v - v_{\mathrm{d}})^2}{R}. \end{aligned} \tag{8}$$

With the control law Eq. (5), we obtain

$$\frac{\mathrm{d}\mathcal{H}_{12}}{\mathrm{d}t} = -k_1(v_{\mathrm{d}}i_1 - vi_{1\mathrm{d}})^2 - k_2E(i_2 - i_{2\mathrm{d}})^2 - \frac{(v - v_{\mathrm{d}})^2}{R}, \tag{9}$$

which shows that $\mathcal{H}_{12}$ decreases monotonically. Therefore, the desired storage function $\mathcal{H}_{12}$ can be a candidate of Lyapunov function for the parallelized system described as Eq. (2) with the control law Eq. (5). It ensures the asymtotic stability around $[i_1\, i_2\, v] = [i_{1\mathrm{d}}\, i_{2\mathrm{d}}\, v_{\mathrm{d}}]$.

We have shown that individual application of PBC to each converter can also stabilize the parallelized system. This is due to the passivity of the whole system. Note that the discussion owes to the ideal setting of circuit elements. Hence, we must take the nonideality into account when we apply these control laws to the practical converters.

3. Numerical Simulation

In this section, we will examine the characteristics of the parallelized system with PBC. The result focuses on the dependence on control gains k_1 and k_2, which govern both the steady state and the transient of the system.

3.1 Setups of Simulation

In the simulation, the circuit is modeled using MATLAB/SIMULINK. Here, we introduce the parameters of circuit elements listed in Table 1. Those resistances are all parasitic resistances except for the load R and are considered to be connected in series to each element. They correspond to the elements in the experiments.

In the simulation, the duty ratios of each converter, μ_1 and μ_2, are estimated by Eq. (5). The switches are also nonideal having a discrete on and off states, so we must have an A/D conversion method maintaining the calculated on and off ratio. PWM is widely used due to its simplicity and easy implementation. However, according to the increase of switching frequency, it must require a significantly fast clock speed of the controller to maintain its resolution of the pulse width. Therefore, we adopt a pulse density modulation, from the expectation of increased switching speed. One of the modulations is $\Delta\Sigma$ modulation. Substituting $\Delta\Sigma$ modulation, the averaged characteristics of DC-DC converters is kept at sufficiently large frequency [16]. In the following simulation, the pulse width is fixed at 1 μs for both converters.

With the aforementioned circuit and controller settings, we consider the supplied power adjustment. While the desired output voltage stays unchanged, the desired input current of each converter is modified. The target is set initially as shown in Table 2. At the instance $t = 0$, we will give a step like change to the target to be shown in Table 3, which is chosen not to alter the power consumption of the whole system.

The elements we have used in the simulation are nonideal, which makes it difficult for us to obtain the exact values of the steady state. Here, we have considered exclusively the diode's voltage drop v_{on} (= 1.35 V) and its power consumption. Hence, the target depends on the relationship

$$\begin{cases} \mu_{1d} = 1 - \dfrac{E_1}{v_d + v_{on}}, \\ \mu_{2d} = \dfrac{v_d + v_{on}}{E_2 + v_{on}}, \\ E_1 i_{1d} + \mu_{2d} E_2 i_{2d} = \dfrac{{v_d}^2}{R} + (1 - \mu_{1d}) v_{on} i_{1d} \\ \qquad\qquad + (1 - \mu_{2d}) v_{on} i_{2d}. \end{cases} \tag{10}$$

However, they do not exactly describe the steady state, because the inner resistances are out of consideration. Therefore, the steady state errors remain. In particular, the desired state with an extremely high boost ratio leads to the significant errors due to the inner resistances with large power consumption. In this case, the error cannot be compensated by the feedback control. So that the decision of the desired state is restricted to have sufficiently low inner power consumption.

Table 1 Circuit parameters.

Element	Product	Values
Inductance L_1	Murata 1447440C	470 μH, 125 mΩ
Inductance L_2	Wurth Elektronik 744137	630 μH, 175 mΩ
Capacitance C_1	CL21-DC250V106	10 μF
Capacitance C_2	Panasonic ECQE2475KF	4.7 μF
Voltage source E_1	Matsusada P4K18-2	9 V
Voltage source E_2	Matsusada P4K36-1	36 V
Load R	0-1614782-1 100RK × 2	50 Ω
Switches	ROHM SCT2450KE	450 mΩ
Diodes	ROHM SCS206AMC	100 mΩ

Table 2 Initial desired state.

v_d	i_{1d}	i_{2d}	μ_{1d}	μ_{2d}
18 V	0.235 A	0.252 A	0.535	0.518

Table 3 Modified desired state.

v_d	i_{1d}	i_{2d}	μ_{1d}	μ_{2d}
18 V	0.548 A	0.108 A	0.535	0.518

3.2 Simulational Results

The steady state characteristics are shown in Figs. 2 and 3. Here, the steady state ripple and the errors of input currents and output voltage are evaluated. Subscripts 'r' and 'e' stand for ripple and error, respectively.

In Figs. 2(a) and 2(b), there appear large ripples when gains are set higher than a certain threshold. It is caused by high gain settings which makes the ripple to be fed unnecessarily to the feedback controller. Also, in Fig. 2(a), the contours are almost parallel to k_2 axis. It means that the ripple of i_1 is independent of k_2. A similar feature can be seen in Fig. 2(b). The ripple of i_2 is independent on k_1. Each gain setting should be set less than its threshold in order to avoid large ripples. The thresholds can be obtained individually because the ripple characteristics were independent.

Figures 2(c) and 2(d) show the error function depending on gains. It is shown that the errors become significantly large at small gain region in which the effect of feedback control is exceedingly reduced. The error can be sufficiently restricted by one of the gains. This is due to the load sharing between the converters. The gains, set larger than the thresholds, cannot keep the error lower due to the saturation of duty ratios or large ripples. The above discussions insist that the gains are limited in a range for appropriate steady state operation.

In Fig. 3, steady state characteristics of the output voltage are shown. Fig. 3(a) is similar to Fig. 2(a). The threshold seen in both figures has almost no difference. It is because the boost converter is more sensitive to output noise than the buck converter. Fig. 3(b) shows a flat surface in the center. This portion corresponds to the appropriate gain settings seen in Fig. 2. It is confirmed that ripple and error characteristics of output voltage and input currents are related.

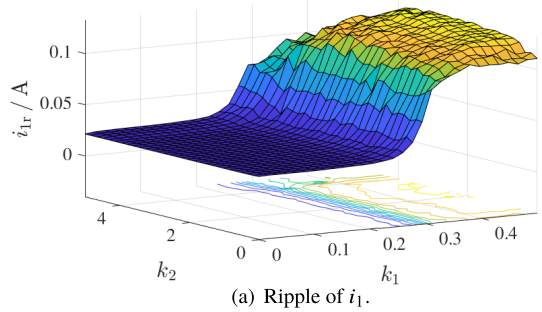

(a) Ripple of i_1.

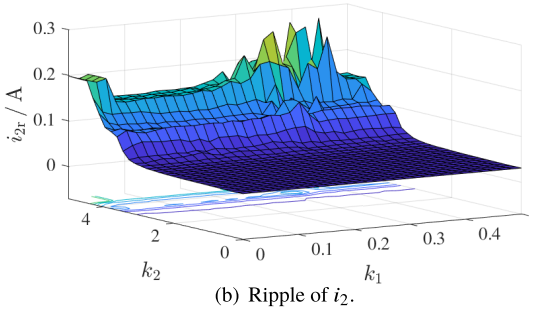

(b) Ripple of i_2.

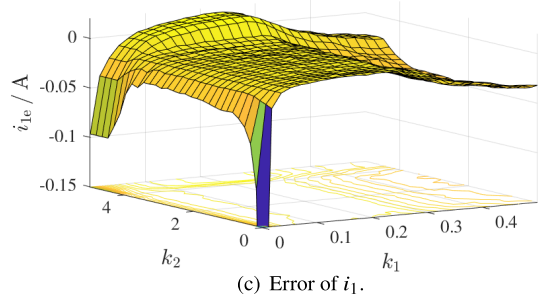

(c) Error of i_1.

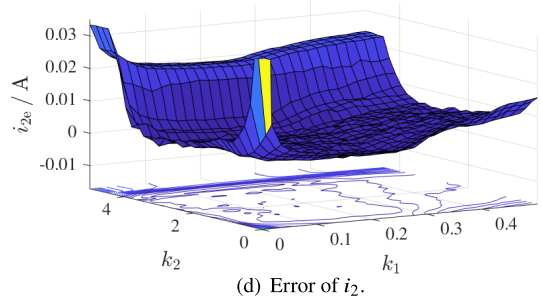

(d) Error of i_2.

Fig. 2 Steady state current characteristics with regards to k_1 and k_2.

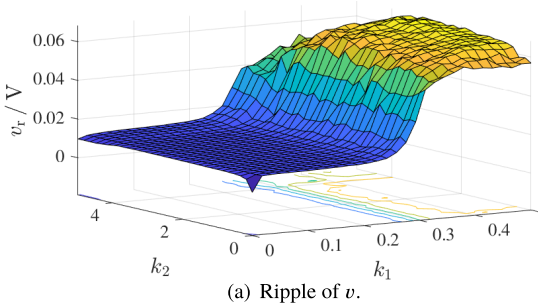

(a) Ripple of v.

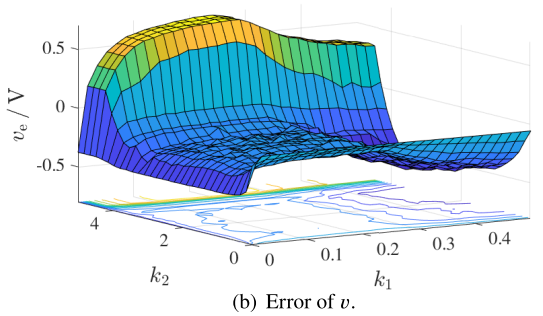

(b) Error of v.

Fig. 3 Steady state voltage characteristics with regards to k_1 and k_2.

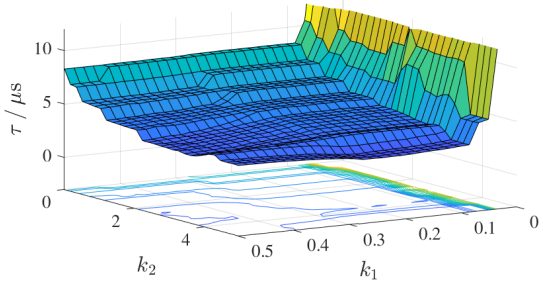

Fig. 4 Surface of time constant τ with regards to k_1 and k_2.

Figure 4 shows the time constant τ of the system. Here, τ is defined as the estimated duration of $\mathcal{H}_{12}$ to be $1/\mathrm{e}$ of initial value. In the figure, the larger gains are set, the smaller τ appears. However, it saturates due to the limit of duty ratio from 0 to 1.

In Fig. 4, the contours are almost parallel to one of the axes. It implies that the time constant of converters is independent of each other. The time constant of the whole system is governed by the slower of the two. These characteristics assure the extension of parallelization into multiple converters.

Figure 5 shows the transient waveforms of i_1 and i_2 for some couples of k_1 and k_2. In Fig. 5(a), it is shown that time for the convergence of i_1 is almost independent of k_2. It corresponds to the results in Fig. 4. The same feature can be seen in Fig. 5(b). In addition, it is confirmed that large gain settings lead to significantly large ripples.

In summary, we have discussed the characteristics of the parallelized system governed by the gains k_1 and k_2. The simulation concludes that both the steady state and transient characteristics of paralleled converters keep independent. Also, it is shown that there is a region of gains for a valid converter operation. This knowledge is applied to the design of paralleled converter systems. In the next section, the parameter in the region will be examined in experiments.

Note that these results are obtained for a fixed circuit parameter and the desired state. The region of the feedback gains for a valid converter operation definitely depends on the circuit parameters and the desired states. Though they are not examined here, it is expected that they might have a region for achieving similar results. From the numerical results and discussions in this section, it is anticipated that the region

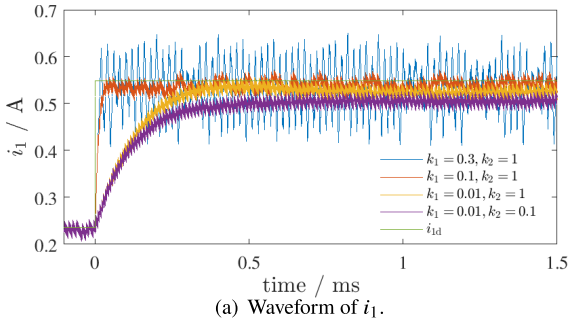

(a) Waveform of i_1.

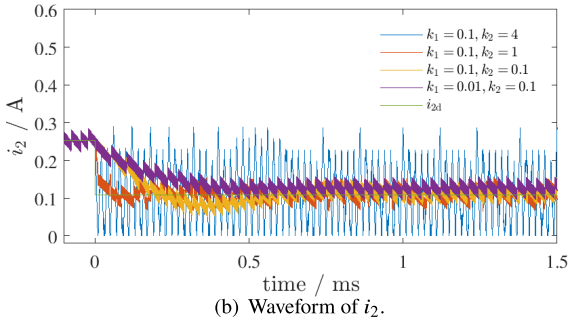

(b) Waveform of i_2.

Fig. 5 Transient characteristics of currents.

of the circuit parameters and the desired states would have a relationship particularly to internal power consumption and output capacitance.

4. Experimental System and Results

In this section, the experimental results of the parallelized system are shown. Supplied power is adjusted corresponding to the simulation. The target states are adopted as shown in Tables 2 and 3.

4.1 Settings of Experiment

Figure 6 shows the photo of experimental system. The parallel system with boost and buck converters are implemented with elements shown in Table 1. Here, current sensors are adopted to measure inductor currents of converters. They are Analog Devices LTC6102 for the boost converter and LEM LTS6-NP for the buck converter. The measured currents are applied for feedback control. Furthermore, the main switches of the converters are driven by the gate driver Silicon Labs SI823BB.

In the experiment, myRIO FPGA is used as the controller to calculate the duty ratio and to generate the switching signal. The duty ratio is calculated according to Eq. (5). The feedback gains are set at $k_1 = 0.03$ and $k_2 = 1$. The switching signal is generated based on the duty ratio by $\Delta\Sigma$ modulation, which is applied to the gate driver.

4.2 Experimental Results

Both the experimental and simulational results are shown in Fig. 7. In the figure, i_1, i_2, and v are shown as the waveforms

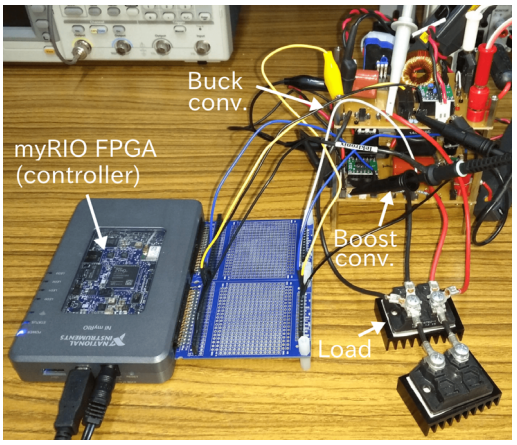

Fig. 6 Photo of the experimental system.

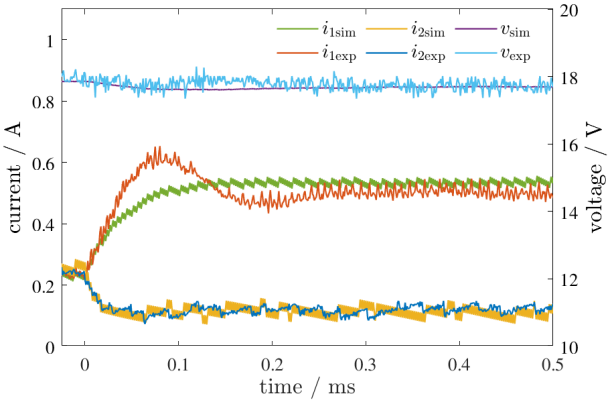

Fig. 7 Experimental and simulation result of a parallelized system.

obtained in the experiment. The subscription 'sim' and 'exp' stand for simulation and experiment, respectively.

At the steady state, it is shown that the experimental system becomes stable. The results well coincide with the simulation after the adjustment of input power. Current i_1 shows a larger error at steady state. It is found to be caused by the parasitic resistances and low gain setting.

At the transient, the experimentally obtained i_1 shows overshoots in waveforms, which are not observed in the corresponding simulation. This is due to the sensor characteristics. The quick response time or the low-pass characteristics of the sensor may possibly cause overshoots or even instability with large gain settings. The low gain setting was appropriate. In order to avoid this conflict, a sufficiently quick response is requested to the sensors.

On the other hand, buck converter current i_2 showed the good coincidence of simulation and experimental results. This clearly shows the independent characteristics, in that the overshoot of i_1 did not affect the transient of i_2. The experimental result also showed that their transient waveforms are governed by their individual time constant.

The simulation and experimental results of output voltage v also well coincide. During the transient, v almost shows no fluctuation from the steady state, due to sufficient

output capacitance. Therefore, the interaction among the converters is reduced since the interconnection between the converters is limited. The independency of the converters are achieved from the circuit parameters as well as control technique.

5. Conclusion

Parallelization of boost and buck converter and their PBC were examined numerically and experimentally. Individual application of PBC to the boost and buck converters achieved asymptotical stabilization of the parallelized system. Through numerical simulation, the dependence on the feedback gains was investigated in terms of ripple characteristics, error characteristics, and time constant. It was concluded that the gain settings were found for steady state operation. It was also confirmed that each converter had independent characteristics. Stability and independent characteristics were also confirmed through the experiment. These results enable the design for more diverse parallelization of converters.

Acknowledgments

This work was partially supported by the Super Cluster Program from Japan Science and Technology Agency. The authors would like to thank Dr. Takafumi Okuda for his support in the experiment. The author, YM, acknowledges Mr. Manuel Sanchez for his support in programming myRIO FPGA.

References

[1] N. Kannan and D. Vakeesan, "Solar energy for future world: - A review," Renewable and Sustainable Energy Reviews, vol.62, pp.1092–1105, 2016.
[2] J.B. Goodenough and K.S. Park, "The Li-ion rechargeable battery: A perspective," J. Am. Chem. Soc., vol.135, no.4, pp.1167–1176, 2013.
[3] T. Ackermann, G. Andersson, and L. Söder, "Distributed generation: A definition," Electr. Pow. Syst. Res., vol.57, no.3, pp.195–204, 2001.
[4] G. Pepermans, J. Driesen, D. Haeseldonckx, R. Belmans, and W. D'haeseleer, "Distributed generation: Definition, benefits and issues," Energ. Policy, vol.33, no.6, pp.787–798, 2005.
[5] Y. Huang and C.K. Tse, "Circuit theoretic classification of parallel connected dc-dc converters," IEEE Trans. Circuits Syst. I, Reg. Papers, vol.54, no.5, no.5, pp.1099–1108, 2007.
[6] H. Matsuo, F. Kurokawa, T. Shigemizu, and N. Watanabe, "Characteristics of the multiple-input dc-dc converter," IEEE Trans. Ind. Electron., vol.51, no.3, pp.625–631, June 2004.
[7] R. Ortega, A.J. Van Der Schaft, I. Mareels, and B. Maschke, "Putting energy back in control," IEEE Control Syst. Mag., vol.21, no.2, pp.18–33, April 2001.
[8] H. Sira-Ramirez, R. Perez-Moreno, R. Ortega, and M. Garcia-Esteban, "Passivity-based controllers for the stabilization of dc-to-dc power converters," Automatica, vol.33, no.4, pp.499–513, 1997.
[9] R. Ortega, J. Perez, P. Nicklasson, and H. Sira-Ramirez, Passivity-based Control of Euler-Lagrange Systems: Mechanical, Electrical and Electromechanical Applications, Communications and Control Engineering, Springer-Verlag, 1998.
[10] H. Sira-Ramirez and R. Silva-Ortigoza, Control Design Techniques in Power Electronics Devices, 2006 ed., Springer-Verlag, 2006.
[11] C. Desoer and E. Kuh, Basic Circuit Theory, McGraw Hill international editions: Electrical and electronic engineering series, McGraw-Hill, 1969.
[12] T. Hikihara and Y. Murakami, "Regulation of parallel converters with respect to stored energy and passivity characteristics," IEICE Trans. Fundamentals, vol.E94-A, no.3, pp.1010–1014, March 2011.
[13] R. Manohar and T. Hikihara, "Dynamic behaviour of a ring coupled boost converter system with passivity-based control," CoRR, vol.abs/1810.00417, 2018.
[14] G. Escobar, A.J. Van der Schaft, and R. Ortega, "A Hamiltonian viewpoint in the modeling of switching power converters," Automatica, vol.35, no.3, pp.445–452, 1999.
[15] A. Isidori, Nonlinear Control Systems, 3rd ed., Springer-Verlag, Berlin, Heidelberg, 1995.
[16] S.K. Dunlap and T.S. Fiez, "A noise-shaped switching power supply using a delta-sigma modulator," IEEE Trans. Circuits Syst. I, Reg. Papers, vol.51, no.6, pp.1051–1061, 2004.

Appendix: Derivation of Control Laws

State averaging model and definition of the shaped energy function will follow the works [8]–[10], [14].

A.1 Boost Converter

Consider a boost converter circuit shown in Fig. A· 1, which has a function of stepping up the voltage at the output. The differential equations describing the circuit are

$$\begin{cases} L_1 \dot{i}_1 = -(1-\mu_1)v + E_1, \\ C_1 \dot{v} = (1-\mu_1) i_1 - \dfrac{v}{R}, \end{cases} \tag{A· 1}$$

where state $u_1 \in \{0, 1\}$ is already replaced with duty ratio $\mu_1 \in [0, 1]$.

The desired state $[i_1\, v] = [i_{1\mathrm{d}}\, v_\mathrm{d}]$ and corresponding desired duty ratio $\mu_1 = \mu_{1\mathrm{d}}$ have to satisfy

$$\begin{cases} \mu_1 = 1 - \dfrac{E_1}{v}, \\ E_1 i_1 = \dfrac{v^2}{R}, \end{cases} \tag{A· 2}$$

which are obtained by setting the left hand side of Eq. (A· 1) to zero.

Desired storage function of the boost converter is defined as

$$\mathcal{H}_1(i_1,\, v) = \frac{1}{2} L_1 (i_1 - i_{1\mathrm{d}})^2 + \frac{1}{2} C (v - v_\mathrm{d})^2, \tag{A· 3}$$

which is shaped to have a minimum at the desired state. By differentiating this storage function $\mathcal{H}_1$ along the trajectory of the boost converter described as Eq. (A· 1), we obtain

$$\begin{aligned} \frac{\mathrm{d}\mathcal{H}_1}{\mathrm{d}t} &= \frac{\partial \mathcal{H}_1}{\partial i_1}\frac{\mathrm{d}i_1}{\mathrm{d}t} + \frac{\partial \mathcal{H}_1}{\partial v}\frac{\mathrm{d}v}{\mathrm{d}t} \\ &= -\frac{(v - v_\mathrm{d})^2}{R} + (\mu_1 - \mu_{1\mathrm{d}})\,(v_\mathrm{d} i_1 - v i_{1\mathrm{d}}). \end{aligned} \tag{A· 4}$$

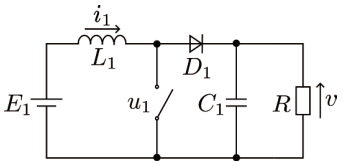

Fig. A· 1 Boost converter.

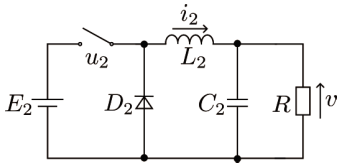

Fig. A· 2 Buck converter.

The first term of the right side stands for the dissipation and the second for the supplied power. Eq. (A· 4) indicates that the boost converter system is a passive system with respect to the shaped storage function $\mathcal{H}_1$, regardless of μ_1.

Regulating the supplied power to be minus ensures the convergence of $\mathcal{H}_1$ at the minimum value zero. Such regulation will be attained by the control law

$$\mu_1 = \mu_{1\mathrm{d}} - k_1(v_\mathrm{d} i_1 - v i_{1\mathrm{d}}) \quad (k_1 > 0), \tag{A· 5}$$

where k_1 is a positive constant. By applying Eq. (A· 5), $\mathcal{H}_1 < 0$ at $[i_1\ v] \neq [i_{1\mathrm{d}}\ v_\mathrm{d}]$ is guaranteed. The desired storage function $\mathcal{H}_1$ becomes a Lyapunov function for the boost converter system. Therefore, asymptotic stability around $[i_1\ v] = [i_{1\mathrm{d}}\ v_\mathrm{d}]$ is achieved. Here, the constant value k_1 is a feedback gain.

A.2 Buck Converter

Consider a buck converter circuit shown in Fig. A· 2. Compared to a boost converter, it has the same elements but has a different topology making it have a different function of stepping the voltage down at the output.

The differential equations describing the buck converter are

$$\begin{cases} L_2 \dot{i}_2 = -v + \mu_2 E_2, \\ C_2 \dot{v} = i_2 - \dfrac{v}{R}, \end{cases} \tag{A· 6}$$

where averaging has already taken place.

By setting the differential terms to zero, the steady state equation will be

$$\begin{cases} \mu_2 = \dfrac{v}{E_2}, \\ i_2 = \dfrac{v}{R}. \end{cases} \tag{A· 7}$$

The desired state $[i_2\ v] = [i_{2\mathrm{d}}\ v_\mathrm{d}]$ and the desired duty ratio $\mu_2 = \mu_{2\mathrm{d}}$ have to be determined to satisfy Eq. (A· 7).

The desired storage function is defined as

$$\mathcal{H}_2(i_2,\ v) = \frac{1}{2}L(i_2 - i_{2\mathrm{d}})^2 + \frac{1}{2}C_2(v - v_\mathrm{d})^2, \tag{A· 8}$$

which is shaped to have a minimum value zero at the desired state. Differentiating this storage function $\mathcal{H}_2$ along the trajectory of the buck converter system described as Eq. (A· 6) gives

$$\begin{aligned} \frac{\mathrm{d}\mathcal{H}_2}{\mathrm{d}t} &= \frac{\partial \mathcal{H}_2}{\partial i_2}\frac{\mathrm{d}i_2}{\mathrm{d}t} + \frac{\partial \mathcal{H}_2}{\partial v}\frac{\mathrm{d}v}{\mathrm{d}t} \\ &= -\frac{(v - v_\mathrm{d})^2}{R} + (\mu_2 - \mu_{2\mathrm{d}})\,E_2(i_2 - i_{2\mathrm{d}}). \end{aligned} \tag{A· 9}$$

The buck converter is shown to be a passive system with respect to a shaped storage function $\mathcal{H}_2$. Here, applying the control law

$$\mu_2 = \mu_{2\mathrm{d}} - k_2(i_2 - i_{2\mathrm{d}}) \quad (k_2 > 0), \tag{A· 10}$$

ensures $\mathcal{H}_2 < 0$ at $[i_2\ v] \neq [i_{2\mathrm{d}}\ v_\mathrm{d}]$. Hence, $\mathcal{H}_2$ becomes a Lyapunov function, which guarantees the asymptotic stability around $[i_2\ v] = [i_{2\mathrm{d}}\ v_\mathrm{d}]$.

Yuma Murakawa received his B.S. degrees in Electrical Engineering from Kyoto University, Japan in 2018. He is currently a graduate student at the Department of Electrical Engineering, Kyoto University. His research interests include power conversion and control.

Yuhei Sadanda received the B.S. and M.S. degrees in Electrical Engineering from Kyoto University in 2015 and 2017, respectively. He is now with Kawasaki Heavy Industries, Ltd.

Takashi Hikihara received PhD from Kyoto University on 1990. Since 1997 he has been a faculty of Department of Electrical Engineering at Kyoto University, where he is currently a Professor. He is also Director General of Kyoto University Library Network. His research interests are including nonlinear science, engineering applications of nonlinear dynamics, power electronics, and sensor network. He is a member of the IEEE, APS, SIAM, ISICE, and IEE, Japan.